ACS OMEGA
http://pubs.acs.org/journal/acsodf
Article

Degradation of Methylene Blue with a Cu(II)−Quinoline Complex Immobilized on a Silica Support as a Photo-Fenton-Like Catalyst

Teerawat Khudkham, Duangdao Channei, Bussaba Pinchaipat, and Ratanon Chotima*

Cite This: *ACS Omega* 2022, 7, 33258−33265

ABSTRACT: A Cu(II)−quinoline complex immobilized on a silica support was prepared to enhance the degradation of dyes. Mesoporous silica functionalized with this Cu(II) complex was turned into a photo-Fenton-like catalyst. Various techniques were used to characterize the resulting material, and the catalytic activity was determined by the degradation of methylene blue (MB) under UV light irradiation. The Cu(II) ion was successfully coordinated to the quinoline ligand on a silica support. The dye degradation investigation has shown that 95% of the dye was degraded in 2.5 h. The active radical species involved in the reaction were $OH^{\bullet}$ and $O_2^{\bullet-}$, suggesting that a peroxo complex intermediate might be formed during degradation processes.

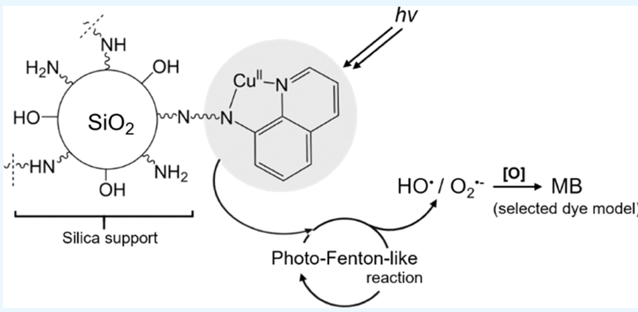

1. INTRODUCTION

A dye is usually an organic or inorganic compound giving color to substrates such as food, fabric, textile cloth, paper, or plastic.[1] The worldwide production of dyes is over 700,000 tons per year.[2−4] About 1−20% of the total world production of dyes is lost during the dyeing process and is released in the textile effluents.[5−8] The washed-out dyes can potentially contaminate natural water and the ecosystem. In recent years, advanced oxidation processes (AOPs) have been used for wastewater treatment. The in situ generation of $HO^{\bullet}$ is the basic principle of this process.[9,10] One promising AOP is the Fenton reaction. The Fenton reaction uses iron ions (Fe^{2+}/Fe^{3+}) as the catalysts in the presence of H_2O_2. It was reported that the Fenton reaction has a high performance and simple method of operation at room temperature.[11,12] However, a limitation of the Fenton reaction is the operational pH range of 2−4.[13] To overcome this disadvantage, an improvement of the Fenton reaction has been investigated. Copper ions have been reported as an alternative for iron ions in the Fenton reaction having the advantage of working over a broader pH range (3−7).[14] In addition, the coordination of copper ions with organic acids, pyridine, amino acids, and chelating agents in solution systems has been shown to enhance the generation of $HO^{\bullet}$.[15−17] Furthermore, extra reactions of the Cu-based Fenton catalyst can occur with photo assistance. For example, light can induce the decrease of the oxidation number of Cu(II)−Cu(I) through ligand to metal charge transfer (LMCT), which is followed by the generation of $HO^{\bullet}$ for the decomposition of substrates.[18] The aim of this research is to investigate a new photo-Fenton-like catalyst. Inspired by copper complexes with organic ligands, quinoline was used as a ligand to form a complex with a Cu(II) ion and immobilized onto a modified silica for the decomposition of methylene blue (MB). The obtained catalyst was investigated by spectroscopic techniques and morphology methods. The catalytic performance of the prepared catalyst was determined from studies of MB degradation under the selected experimental conditions, including catalyst dosage, H_2O_2 concentration, time, and the UV light irradiation effect.

2. RESULTS AND DISCUSSION

2.1. Catalyst Synthesis and Characterization. The SiO_2 used in this work was amorphous silica, showing a broad peak at 22° (Figure S1) in its X-ray diffraction (XRD) spectra.[19] After the surface modifications, only characteristic peaks in the infrared (IR) region of silica were observed (Figure S2) in the FTIR spectra. This is due to the fact that the concentration of (3-aminopropyl) triethoxysilane (APTES) and the Cu(II)−quinoline complex was too low when compared with the amount of silica.[20] The SiO_2 was spherical with different degrees of aggregation and dimensions smaller than 100 nm (Figure 1) as the reaction was performed with a high concentration of water (14 mol L^{-1}). In addition, the concentration of ammonia was relatively low (1.4 mol L^{-1}) to inhibit the aggregation of the nascent silica particles.[21] No change in morphology of the silica particles was observed as a

Received: June 16, 2022
Accepted: September 1, 2022
Published: September 8, 2022

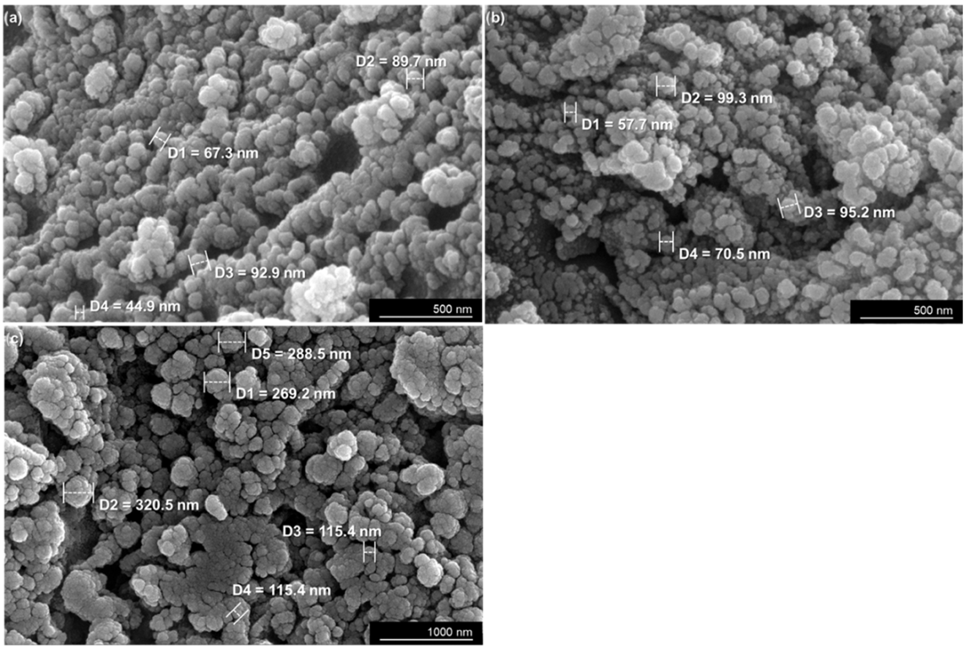

Figure 1. SEM images of (a) SiO_2, (b) SiO_2−NH_2, and (c) SiO_2−Cu(II)−quinoline complexes.

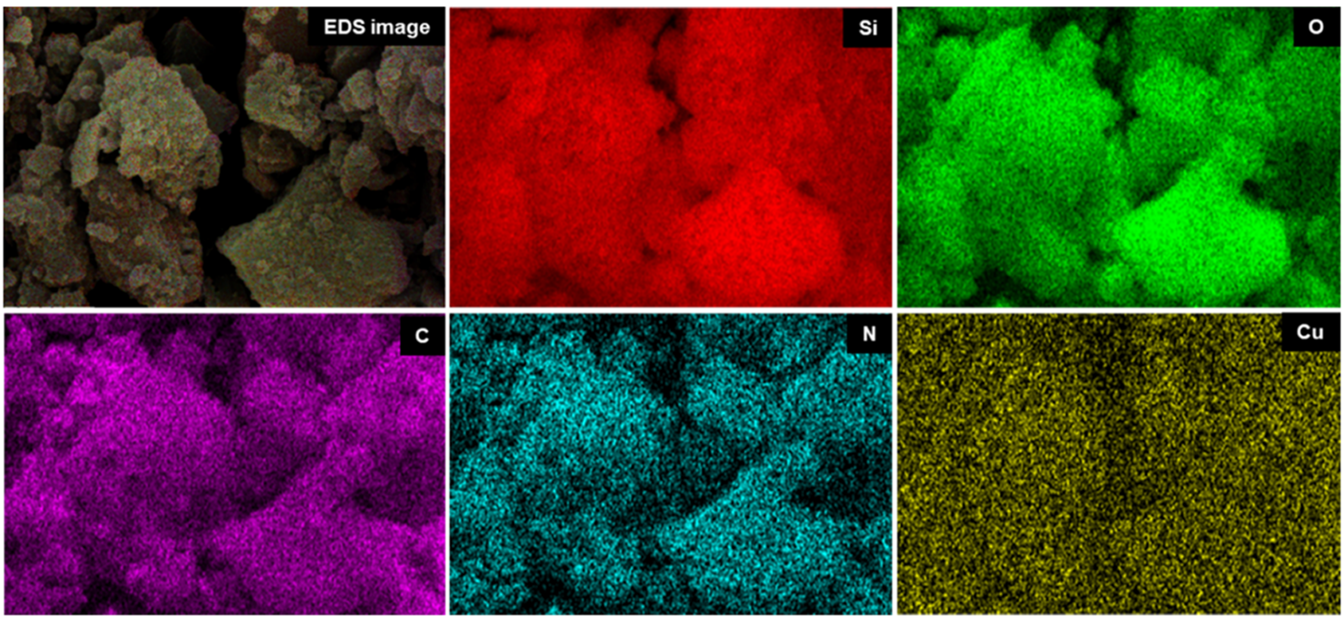

Figure 2. EDX mapping of the SiO_2−Cu(II)−quinoline complex.

result of the modifications and only more extensive aggregation of the silica particles was observed.

The elemental mapping performed by energy dispersive X-ray spectroscopy (EDX) demonstrated that all elements in the catalyst were uniformly distributed on the silica surface (Figure 2). Two peaks of Cu at 0.930 and 8.040 keV provide key evidence that there is Cu present in the silica (Figure 3). The total Cu content was found to be 0.6 wt % in the selected area.

Adsorption−desorption isotherm for the different materials was measured and is shown in Figure 4. The specific surface area (S_{BET}) was calculated using the Brunauer−Emmett−Teller (BET) equation. As shown in Table 1, the S_{BET} of SiO_2 (527.3 $m^2\ g^{-1}$) decreased to 216.4 and 103.6 $m^2\ g^{-1}$ in SiO_2−NH_2 and SiO_2−Cu(II)−quinoline complexes, respectively.

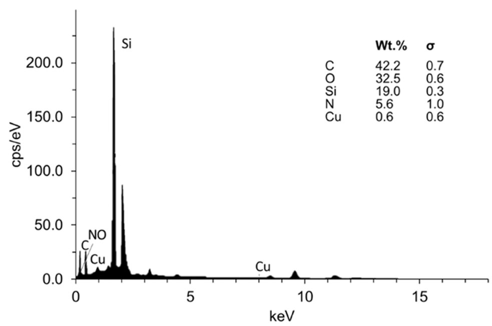

Figure 3. EDX spectra of the SiO_2−Cu(II)−quinoline complex.

https://doi.org/10.1021/acsomega.2c03770
ACS Omega 2022, 7, 33258−33265

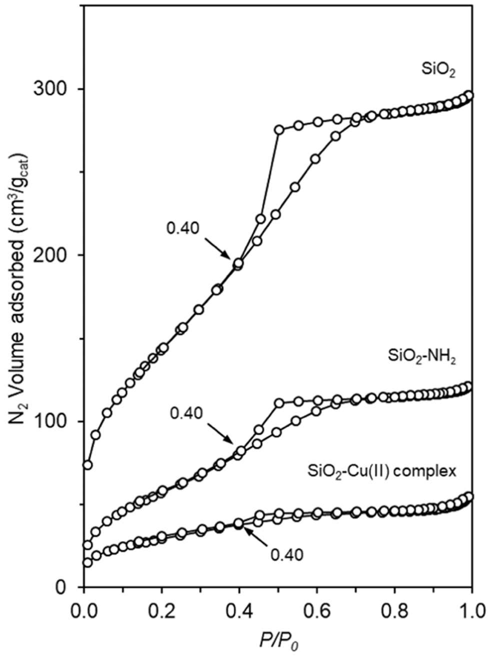

Figure 4. N_2 adsorption−desorption isotherms of SiO_2, SiO_2−NH_2, and SiO_2−Cu(II) complexes.

Table 1. Textural Properties of SiO_2, SiO_2−NH_2, and SiO_2−Cu(II) Complexes

sample	S_{BET} ($m^2\ g^{-1}$)	V_{pmeso} ($cm^3\ g^{-1}$)	pore size distribution (nm)
SiO_2	527.3	0.41	3.36
SiO_2−NH_2	216.4	0.16	3.23
SiO_2−Cu(II)−quinoline complex	103.6	0.050	2.97

Pore volume (V_{pmeso}) and pore size distributions were obtained by the Barrett−Joyner−Halenda (BJH) model. The values of these parameters also decrease and remain in the characteristic ranges of mesoporous materials.[22]

X-ray photoelectron spectroscopy (XPS) spectra of SiO_2−quinoline before and after loading with Cu(II) are shown in Figure 5a. Peaks of Si 2p, C 1s, N 1s, and O 1s can be observed at bonding energy (BE) values of 103, 285, 399, and 532 eV, respectively. The comparison of the survey spectra of SiO_2−quinoline before and after loading Cu(II) ions indicates the presence of the Cu element. A new peak of Cu(II) was observed at a binding energy of 935 eV. The value was assigned to the Cu 2p orbital. The strong Cu $2p_{1/2}$ and Cu $2p_{3/2}$ peaks at 952.1 and 932.3 eV were in an agreement with the oxidation state +2 of Cu 2p (Figure 5b). As shown in Figure 5c,d, the high-resolution of the N 1s spectrum fitted with deconvolution peaks of N element reveals peaks at 399.1 eV (primary amines) and 400.1 eV (imines).[23−25] These binding energies (BEs) of the nitrogen atoms were shifted to 399.2 and 400.4 eV, respectively, due to the electron density of N atoms being donated to form a shared bond with Cu(II) ions.[26]

The band gap of SiO_2 and SiO_2−Cu(II) complexes was determined through the Kubelka−Munk function. Figure 6 shows the extrapolation of the linear part of the plot on the energy axis. The observed band gaps were 5.8 and 2.8 eV, respectively. This result indicates that the addition of the Cu(II)−quinoline complex to the silica support decreases the band gap of SiO_2.

2.2. Photo-Fenton-Like Degradation of MB. The catalytic performance of the catalyst was evaluated using the degradation of MB under UV light irradiation over 150 min as a model reaction. The control experiments included MB/cat. (UV) and MB/cat./H_2O_2 (dark), were performed under identical conditions. The time profile of MB degradation over the catalyst in different conditions is illustrated in Figure 7a. The amounts of MB removed after 150 min of experiments MB/cat. (UV) and MB/cat./H_2O_2 were 15.8% and 54, respectively. The best MB removal (95%) was obtained for MB/cat./H_2O_2 (UV). The photocatalytic activity was quantitatively investigated by the calculation of the apparent rate constant (k) of the catalyst using eq 1.

$$-\ln(C^t/C^{30}) = kt \qquad (1)$$

where C_t is the concentration of the MB solution (mg L^{-1}) at the reaction time t, C_{30} is the concentration of the MB solution at 30 min, and k is the apparent reaction rate constant. The slope (k value in min^{-1}) was obtained from the linear plot of $-\ln(C^t/C^{30})$ vs t (min). The k value increased from −0.04 to 0.49 and 2.43 (10^{-2} min^{-1}) (Figure 7b). This result also shows that the reaction rate was enhanced the most in the condition system MB/cat./H_2O_2 (UV).

The changes in the UV−vis spectra of MB of the MB/cat./H_2O_2 (UV) system are shown in Figure 8. The characteristic band of MB (662 nm) decreased dramatically. Also, no new peak was observed, which suggests that the chromophore of MB was decomposed during the reaction.[27]

Further experiments were conducted to determine the effect of H_2O_2 concentration. More extensive degradation with higher k values was observed when the H_2O_2 content was increased (Figure 9a). The degradation efficiency at 2.50 h increased from 15.8 to 95.0%. In addition, k values for MB degradation increased with increasing hydrogen peroxide concentration from −0.07 to 2.35 × 10^{-2} min^{-1} (Figure 9b). This finding suggests that H_2O_2 affects the MB degradation.

There are various radicals involved in the Fenton-based reaction. Important active radical species such as $HO^\bullet$ and $O_2^{\bullet-}$/$HOO^\bullet$ were detected. The type of radical species in the MB degradation was determined using coumarin, isopropyl alcohol (IPA), and *p*-benzoquinone (BQ) as probes. Coumarin is a poorly fluorescent molecule that was used as a probe for the detection of the $HO^\bullet$ radical. It produces the highly fluorescent compound 7-hydroxycoumarin upon the reaction with $HO^\bullet$ radicals. The amount of 7-hydroxycoumarin reflects the amount of $HO^\bullet$ generated in the system. The fluorescent spectra of the reaction mixture recorded at different time points (0−150 min) are shown in Figure 10. After exposing the reaction mixture to UV light for 30 min (60 min of total reaction time), coumarin was hydroxylated to 7-hydroxycoumarin confirmed by the strong emission band at 460 nm. The band increased continuously with increasing exposure time. These results suggest that the $HO^\bullet$ radical was generated in the conditions of cat./H_2O_2 under UV irradiation.

Furthermore, results of radical trapping experiments are shown in Figure 11. The degradation of MB was not interrupted by the addition of $HO^\bullet$ radical scavenger isopropyl alcohol (IPA). However, the $HO^\bullet$ radical was still involved in MB degradation, as confirmed by the production of 7-hydroxycoumarin. On the other hand, $O_2^{\bullet-}$ trapping by *p*-

https://doi.org/10.1021/acsomega.2c03770
ACS Omega 2022, 7, 33258−33265

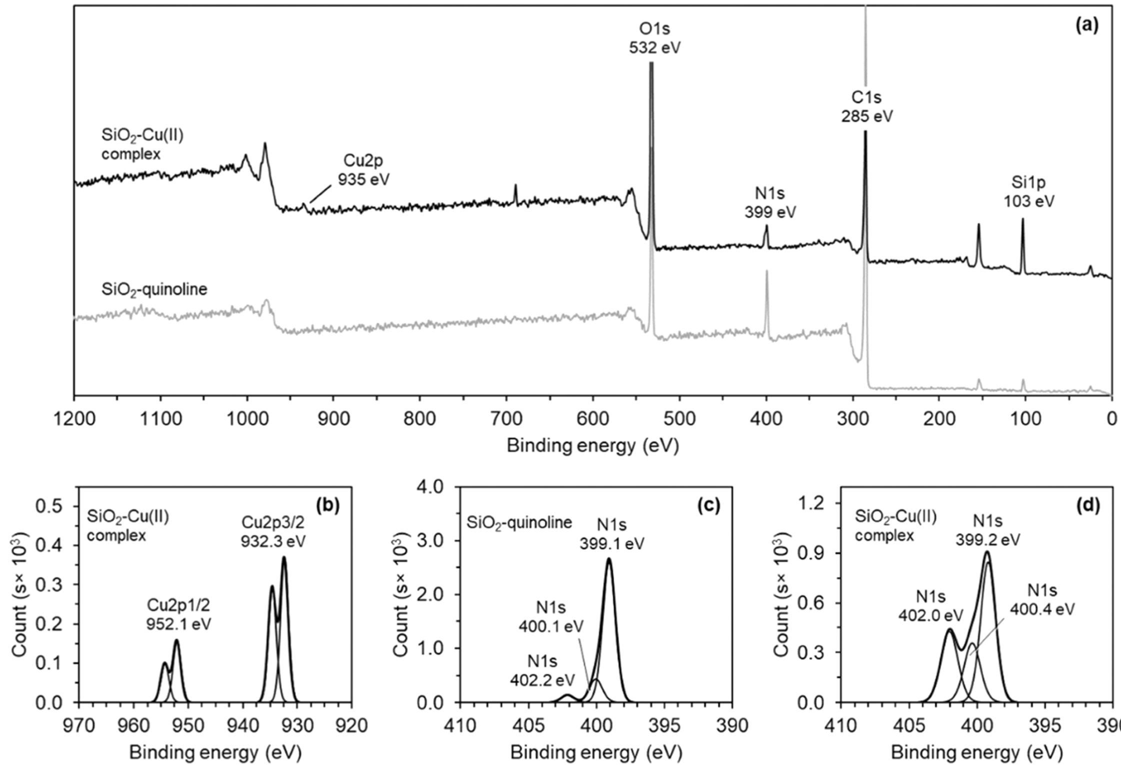

Figure 5. (a) XPS survey spectra of SiO_2−quinoline before and after loading of Cu(II), and the high-resolution XPS for (b) Cu 2p and N 1s (c) before and (d) after loading of Cu(II).

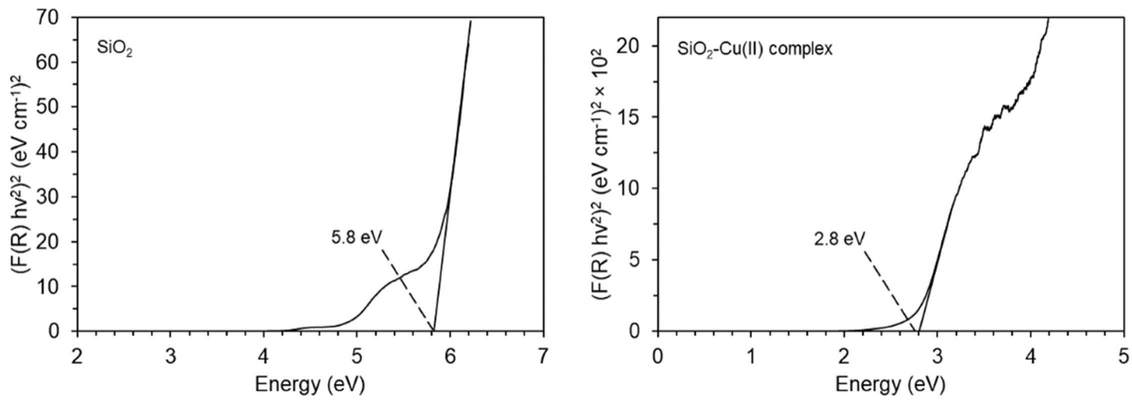

Figure 6. Kubelka−Munk function of (a) SiO_2 and (b) SiO_2−Cu(II)−quinoline complexes.

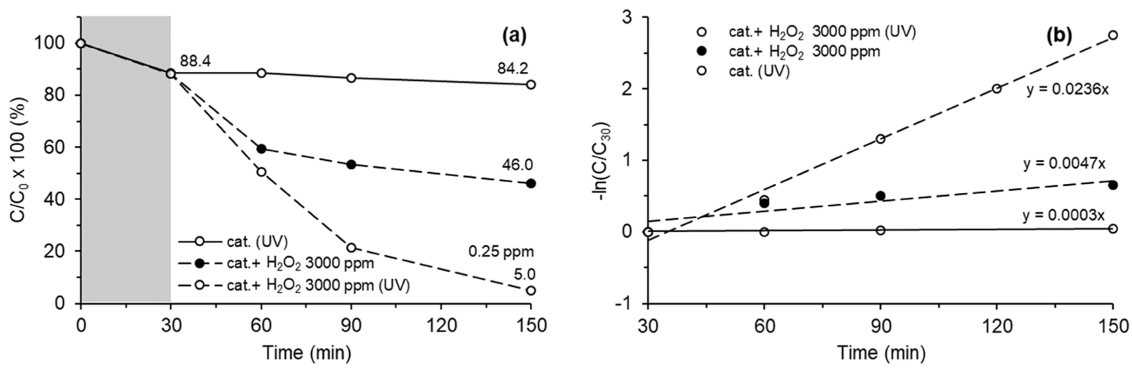

Figure 7. (a) Catalytic efficiency and (b) pseudo-first-order kinetic plot for the degradation of MB in different reaction systems.

benzoquinone (BQ) shows competitiveness with MB degradation.

The results are in accordance with the radical generation by the Cu(II)/organic ligand/H_2O_2 system, which simultaneously

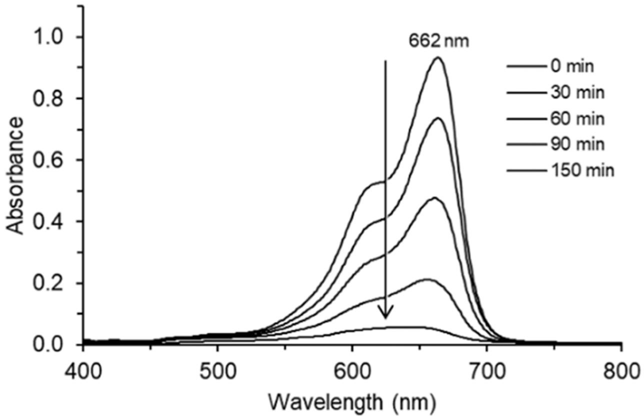

Figure 8. Changes in the spectra of MB.

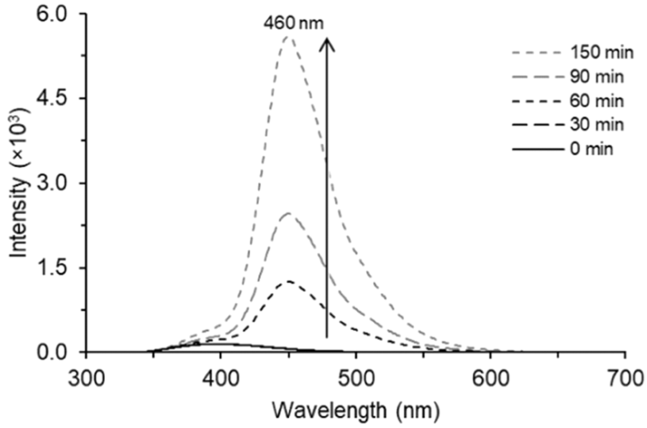

Figure 10. Changes in the fluorescence spectra of coumarin from 0 to 150 min.

generates $HO^{\bullet}$ and $O_2^{\bullet -}/HOO^{\bullet}$ radicals via a complex mechanism forming a peroxo complex.[28] Therefore, the mechanism of the catalyst function in the photo-Fenton-like reaction is proposed in Scheme 1.[29] The catalysis takes place on the surface of the silica particles, where the active site of the [L−Cu^{2+}] complex was immobilized. The unsaturated [L−Cu^{2+}] complex could bind peroxide to form [L−Cu^{2+}($^{-}O_2H$)] (pathway (1)), which can subsequently transform into a peroxo complex [L−Cu^{+}(O_2H)$^{\bullet}$] as a result of charge transfer between a hydroperoxide anion ($^{-}O_2H$) and Cu^{2+} (pathway (2)).[30,31] The peroxo complex can then react with H_2O_2 to produce $HO^{\bullet}$ radicals (pathway (4)).[30−34] The [L−Cu^{2+}($^{-}O_2H$)] can also be regarded as an oxidant based on a complex mechanism, directly oxidizing substrates through pathway (6).[35,36] In addition, the copper redox cycle with $HO^{\bullet}$ and the production of dissolved O_2 (pathway (4)) are likely to involve a catalytic cycle (pathways (7) and (8)).[20,37−41] During these processes, the substrate in the reaction can be excited (pathway (9)), transferring an electron to the metal-centered orbitals (pathway (10)) with this substrate to the metal charge transfer (SMCT) process contributing to the decolorization of the substrate via the loss of conjugation of the double bonds in the molecule.[40] With photo assistance, the photoreduction of Cu^{2+} to Cu^{+} occurs through charge transfer between the ligand and the metal. This is followed by the production of an oxidized ligand (L^{+}) (pathway (11)), which could subsequently oxidize substrate molecules (pathway (13)).

The stability of the catalyst was studied in consecutive photo-Fenton-like reactions for MB degradation. The results of this investigation are shown in Figure S3. A large capacity of adsorption of the catalyst was found after the first reaction run, and the degradation efficiency by the photo-Fenton-like reaction decreased. The apparent rate constants are 3.65×10^{-2} and 1.04×10^{-2} min^{-1} for the first and second reaction runs, respectively. These findings suggest that the catalysis performance could be affected by the leaching of active sites, which may then be decomposed by self-degradation reactions during the MB degradation.[37,42]

3. CONCLUSIONS

A new photo-Fenton-like catalyst was prepared, as evidenced by the reported characterizations. MB was degraded under UV light irradiation in the presence of this catalyst in 2.5 h. However, the catalyst was lost during the catalytic reaction. The development of this type of catalyst for future use remains a challenge, especially in terms of protection from self-degradation, which could be achieved by operating under milder conditions.

4. MATERIALS AND EXPERIMENTAL SECTION

4.1. Materials. All chemicals were used without further purification. Ammonium hydroxide (NH_4OH, 28 wt %), (3-aminopropyl) triethoxysilane (APTES, 99%), 8-aminoquinoline ($C_9H_8N_2$, 98%), ethanol (C_2H_5OH, 99.8%), tetraethyl orthosilicate (TEOS, 98%), isopropanol (IPA, C_3H_8O), glutaraldehyde 25 wt % ($C_5H_8O_2$), glacial acetic acid (CH_3COOH), and coumarin ($C_9H_6O_2$, 99%) were purchased from Sigma-Aldrich. *p*-Benzoquinone (BQ, $C_6H_4O_2$) and hydrogen peroxide 30 wt % (H_2O_2) were purchased from

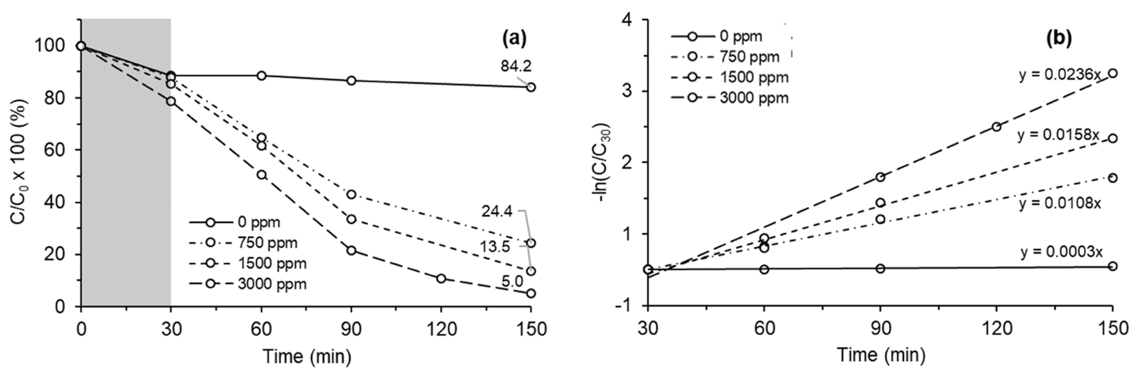

Figure 9. (a) Catalytic efficiency and (b) pseudo-first-order kinetic plot for degradation of MB using different concentrations of H_2O_2.

https://doi.org/10.1021/acsomega.2c03770
ACS Omega 2022, 7, 33258−33265

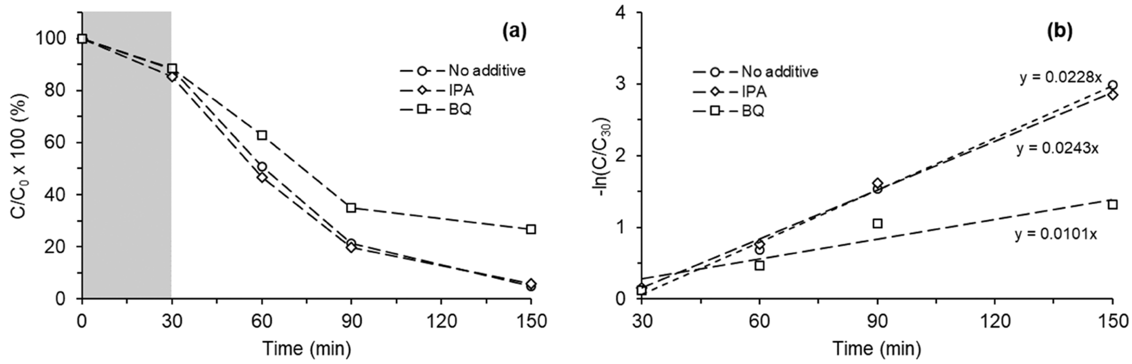

Figure 11. (a) Catalytic efficiency and (b) pseudo-first-order kinetic plot of the catalyst in the presence of radical active species-trapping agents.

Scheme 1. Proposed Mechanism of Action of the Heterogeneous Cu−L Complex Photo-Fenton-Like System

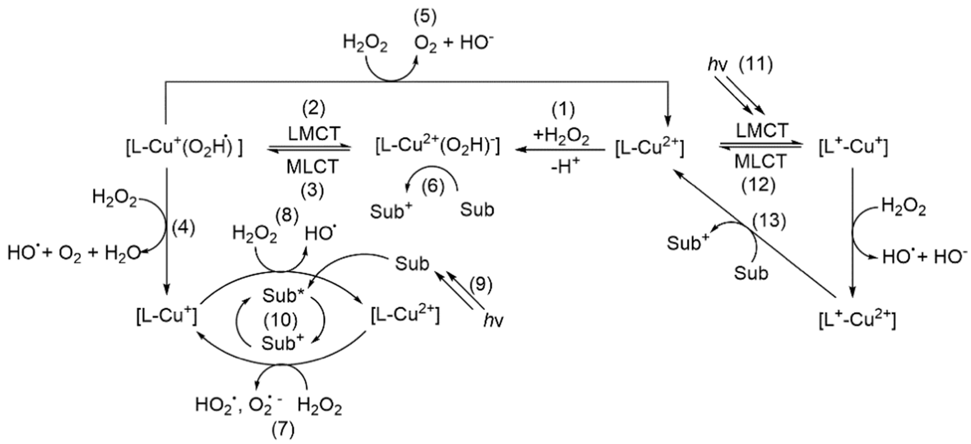

Scheme 2. Synthesis of the Cu(II)−Quinoline Complex on Silica Support

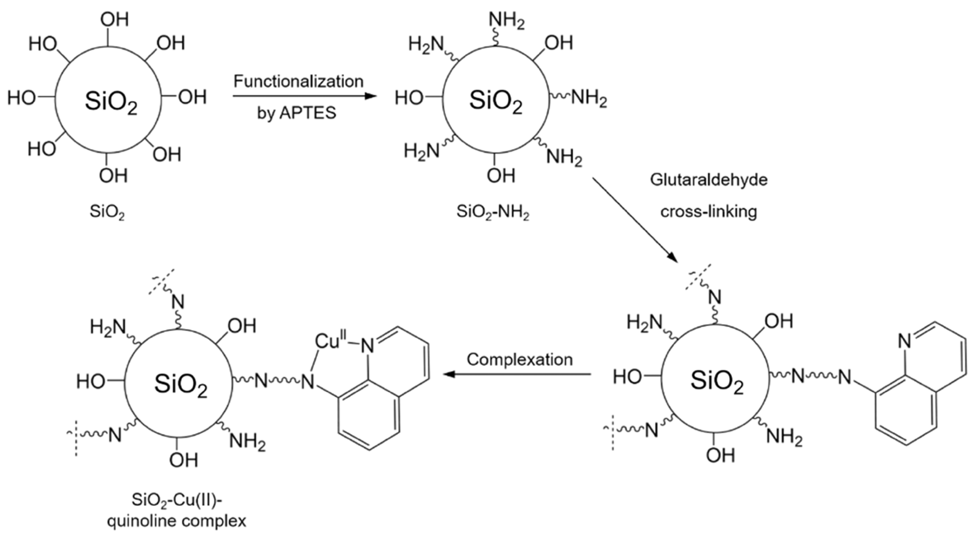

MERCK. Copper(II) sulfate pentahydrate ($CuSO_4 \cdot 5H_2O$, 98%) was purchased from Ajax Finechem. Deionized water (DI) was used throughout the entire experiment.

4.2. Synthesis. The synthesis of the Cu(II)−quinoline complex immobilized on silica is shown in Scheme 2.

4.2.1. Preparation of Silica Support. The silica support was prepared by the hydrolysis of TEOS.[43] A mixture of ethanol (170 mL) and DI water (511 mL) was sonicated for 10 min. This was followed by a dropwise addition of TEOS (7.0 mL) to the reaction mixture under ultrasonication. After 20 min, 28 wt % NH_4OH (12 mL) was added to catalyze the condensation reaction. The reaction mixture was then stirred at 750 rpm for 60 min. Then, the formation of a white turbid suspension was observed. The solid was dried at 100 °C for 5 h and obtained as the silica support (1.8 g). This material was denoted SiO_2.

4.2.2. Preparation of Amine-Functionalized Silica Support. The prepared silica support was dried at 100 °C for 30 min before further use. The dried solid (1.2 g) was dispersed in ethanol (10 mL) and continually stirred at 500 rpm. Then,

https://doi.org/10.1021/acsomega.2c03770
ACS Omega 2022, 7, 33258−33265

APTES (3.6 mmol, 0.84 mL) was slowly added to the suspension. After 30 min, DI water (7.2 mmol, 130 μL) was added to generate the alkoxide groups of APTES. The amount of DI water was twice the amount for complete hydrolysis of APTES.[22] The reaction was continued for further 30 min. The solids (1.1 g) were obtained after drying at 100 °C for 2 h. The prepared amine-functionalized silica was denoted SiO_2-NH_2.

4.2.3. Preparation of the Cu(II)−Quinoline Complex Immobilized on Silica Support. A total of 1.0 g of amine-functionalized silica support (SiO_2-NH_2) was dispersed in DI water (4 mL). Then, the suspension was sonicated for 10 min. 8-Aminoquinoline (432 mg, 3 mmol) dissolved in 5 mL of CH_3CN was slowly added into the suspension. After 30 min, the mixture of glutaraldehyde (2.4 mL, 6 mmol) and glacial acetic acid (0.69 mL, 12 mmol) was added dropwise. The reaction was carried out at room temperature for 12 h. Afterward, 20 mL of a 0.1 M copper(II) sulfate solution was added to the reaction mixture, which was then stirred at 60 °C for 5 h.[20] The product (0.8 g) was collected by centrifugation at 9000 rpm, washed by DI water, and dried at 80 °C for 4 h. The product was denoted the SiO_2−Cu(II)−quinoline complex or catalyst.

4.3. Material Characterization. The surface of the samples was investigated by Fourier transform infrared spectroscopy-attenuated total reflectance (FTIR-ATR, Spectrum GX). The structure and composition were investigated by powder X-ray diffraction (XRD, Panalytical/Expert 2θ: 5−140°). Morphologies were observed by field emission scanning electron microscopy (FESEM, LEO1455VP) equipped with energy-dispersive X-ray spectroscopy (EDX). Specific surface areas of the samples were evaluated by Brunauer, Emmett, and Teller (BET) surface analysis (TriStar II 3020). The elemental composition and the surface chemical state were investigated by X-ray photoelectron spectroscopy (XPS, AXIS Ultra DLD). Characteristic reflectance spectra were obtained by diffuse reflectance spectroscopy (DRS, Agilent 8453). The dye concentration was measured by a UV−vis spectrophotometer (UV-6100 UV/VIS).

4.4. Photocatalytic Experiments. Photocatalytic performance was investigated in a closed chamber with vertical light irradiation. Ambient temperature inside of the chamber was maintained at 28 °C with air cooling. The light source was a 30 W UV lamp, which was placed so that the distance between the level of the solution and the light source was 13 cm. The reactions were carried out in a batch experiment setup to avoid the loss of catalyst dosage. In a typical experiment, 1.0 mg of the catalyst (0.2 g L^{-1}) was added to a 5 ppm solution of MB (5.0 mL) and the mixture was ultrasonicated for 2 min. The reaction was continually stirred in the dark for 30 min to reach adsorption equilibrium (Figure S4). Then, one of the reactions was taken out and centrifuged to obtain a clear supernatant. The MB concentration determined at this point was labeled as C_{30}. After that, 30 wt % H_2O_2 was added to the reaction mixture and the UV lamp was turned on. At predetermined reaction time points (30, 60, and 120 min), the reaction mixture was centrifuged and analyzed. The concentrations of MB were determined from its maximum absorption (664 nm) using a UV−vis spectrometer. Decolorization efficiency of MB was calculated using eq 2.

$$\eta = (1 - C^t/C^0) \times 100\% = (1 - A^t/A^0) \times 100\% \qquad (2)$$

where C_t is the concentration of the MB solution at the reaction time t, C_0 is the initial concentration of the MB solution at 0 min, and A and A_0 are the corresponding absorption values.

■ ASSOCIATED CONTENT

Supporting Information

The Supporting Information is available free of charge at https://pubs.acs.org/doi/10.1021/acsomega.2c03770.

Additional experimental results, including adsorption equilibrium and stability of the catalyst, and XRD, FTIR, and SEM images (PDF)

■ AUTHOR INFORMATION

Corresponding Author

Ratanon Chotima − *Department of Chemistry, Naresuan University, Phitsanulok 65000, Thailand;* orcid.org/0000-0002-8846-8745; Email: ratanonc@nu.ac.th

Authors

Teerawat Khudkham − *Department of Chemistry, Naresuan University, Phitsanulok 65000, Thailand*

Duangdao Channei − *Department of Chemistry, Naresuan University, Phitsanulok 65000, Thailand;* orcid.org/0000-0001-8951-3934

Bussaba Pinchaipat − *Department of Chemistry, Naresuan University, Phitsanulok 65000, Thailand*

Complete contact information is available at: https://pubs.acs.org/10.1021/acsomega.2c03770

Notes

The authors declare no competing financial interest.

■ ACKNOWLEDGMENTS

This work was financially supported by the Development and Promotion of Science and Technology Talents Project (DPST), Royal Thai Government.

■ REFERENCES

(1) Heinz, M.Dyes, General Survey. In *Ullmann's Encyclopedia of Industrial Chemistry*; Wiley-VCH Verlag GmbH & Co., 2014; pp 1−38.

(2) Lee, J.-W.; Choi, S.-P.; Thiruvenkatachari, R.; Shim, W.-G.; Moon, H. Evaluation of the performance of adsorption and coagulation processes for the maximum removal of reactive dyes. *Dyes Pigm.* **2006**, *69*, 196−203.

(3) McMullan, G.; Meehan, C.; Conneely, A.; Kirby, N.; Robinson, T.; Nigam, P.; Banat, I.; Marchant, R.; Smyth, W. Microbial decolourisation and degradation of textile dyes. *Appl. Microbiol. Biotechnol.* **2001**, *56*, 81−87.

(4) Pearce, C. I.; Lloyd, J. R.; Guthrie, J. T. The removal of colour from textile wastewater using whole bacterial cells: a review. *Dyes Pigm.* **2003**, *58*, 179−196.

(5) Konstantinou, I. K.; Albanis, T. A. TiO2-assisted photocatalytic degradation of azo dyes in aqueous solution: kinetic and mechanistic investigations: A review. *Appl. Catal., B* **2004**, *49*, 1−14.

(6) Deng, F.; Min, L.; Luo, X.; Wu, S.; Luo, S. Visible-light photocatalytic degradation performances and thermal stability due to the synergetic effect of TiO2 with conductive copolymers of polyaniline and polypyrrole. *Nanoscale* **2013**, *5*, 8703−8710.

(7) Xu, S.; Zhu, Y.; Jiang, L.; Dan, Y. Visible Light Induced Photocatalytic Degradation of Methyl Orange by Polythiophene/TiO2 Composite Particles. *Water, Air, Soil Pollut.* **2010**, *213*, 151−159.

(8) Wang, D.; Wang, Y.; Li, X.; Luo, Q.; An, J.; Yue, J. Sunlight photocatalytic activity of polypyrrole−TiO2 nanocomposites prepared by 'in situ' method. *Catal. Commun.* **2008**, *9*, 1162−1166.
(9) Wang, J. L.; Xu, L. J. Advanced Oxidation Processes for Wastewater Treatment: Formation of Hydroxyl Radical and Application. *Crit. Rev. Environ. Sci. Technol.* **2012**, *42*, 251−325.
(10) Oturan, M. A.; Aaron, J.-J. Advanced Oxidation Processes in Water/Wastewater Treatment: Principles and Applications. A Review. *Crit. Rev. Environ. Sci. Technol.* **2014**, *44*, 2577−2641.
(11) Bigda, R. J. Consider Fenton's chemistry for wastewater treatment. *Chem. Eng. Prog.* **1995**, *91*, 62−66.
(12) Mesquita, I.; Matos, L. C.; Duarte, F.; Maldonado-Hódar, F. J.; Mendes, A.; Madeira, L. M. Treatment of azo dye-containing wastewater by a Fenton-like process in a continuous packed-bed reactor filled with activated carbon. *J. Hazard. Mater.* **2012**, *237-238*, 30−37.
(13) Ran, J.; Li, X.; Zhao, Q.; Qu, Z.; Li, H.; Shi, Y.; Chen, G. Synthesis, structures and photocatalytic properties of a mononuclear copper complex with pyridine-carboxylato ligands. *Inorg. Chem. Commun.* **2010**, *13*, 526−528.
(14) Nieto-Juarez, J. I.; Pierzchła, K.; Sienkiewicz, A.; Kohn, T. Inactivation of MS2 coliphage in Fenton and Fenton-like systems: role of transition metals, hydrogen peroxide and sunlight. *Environ. Sci. Technol.* **2010**, *44*, 3351−3356.
(15) Verma, P.; Baldrian, P.; Gabriel, J.; Trnka, T.; Nerud, F. Copper−ligand complex for the decolorization of synthetic dyes. *Chemosphere* **2004**, *57*, 1207−1211.
(16) Lázaro Martínez, J. M.; Leal Denis, M. F.; Piehl, L. L.; de Celis, E. R.; Buldain, G. Y.; Campo Dall' Orto, V. Studies on the activation of hydrogen peroxide for color removal in the presence of a new Cu(II)-polyampholyte heterogeneous catalyst. *Appl. Catal., B* **2008**, *82*, 273−283.
(17) Gazi, S.; Ananthakrishnan, R.; Singh, N. D. P. Photodegradation of organic dyes in the presence of [Fe(III)-salen]Cl complex and H2O2 under visible light irradiation. *J. Hazard. Mater.* **2010**, *183*, 894−901.
(18) Masarwa, M.; Cohen, H.; Meyerstein, D.; Hickman, D. L.; Bakac, A.; Espenson, J. H. Reactions of low-valent transition-metal complexes with hydrogen peroxide. Are they "Fenton-like" or not? 1. The case of Cu+aq and Cr2+aq. *J. Am. Chem. Soc.* **1988**, *110*, 4293−4297.
(19) Vinoda, B. M.; Vinuth, M.; et al. Photocatalytic Degradation of Toxic Methyl Red Dye Using Silica Nanoparticles Synthesized from Rice Husk Ash. *J. Environ. Anal. Toxicol.* **2015**, *05*, No. 1000336.
(20) Yuan, W.; Zhang, C.; Wei, H.; Wang, Q.; Li, K. In situ synthesis and immobilization of a Cu(ii)−pyridyl complex on silica microspheres as a novel Fenton-like catalyst for RhB degradation at near-neutral pH. *RSC Adv.* **2017**, *7*, 22825−22835.
(21) Wang, J.; Sugawara-Narutaki, A.; Fukao, M.; Yokoi, T.; Shimojima, A.; Okubo, T. Two-Phase Synthesis of Monodisperse Silica Nanospheres with Amines or Ammonia Catalyst and Their Controlled Self-Assembly. *ACS Appl. Mater. Interfaces* **2011**, *3*, 1538−1544.
(22) Hernández-Morales, V.; Nava, R.; Acosta-Silva, Y. J.; Macías-Sánchez, S. A.; Perez Bueno, J.; Pawelec, B. Adsorption of lead (II) on SBA-15 mesoporous molecular sieve functionalized with −NH2 groups. *Microporous Mesoporous Mater.* **2012**, *160*, 133−142.
(23) Abouliatim, Y.; Chartier, T.; Abelard, P.; Chaput, C.; Delage, C. Optical characterization of stereolithography alumina suspensions using the Kubelka−Munk model. *J. Eur. Ceram. Soc.* **2009**, *29*, 919−924.
(24) Bayazit, M. K.; Clarke, L. S.; Coleman, K. S.; Clarke, N. Pyridine-Functionalized Single-Walled Carbon Nanotubes as Gelators for Poly(acrylic acid) Hydrogels. *J. Am. Chem. Soc.* **2010**, *132*, 15814−15819.
(25) Silva, A. R.; Martins, M.; Freitas, M. M. A.; Figueiredo, J. L.; Freire, C.; de Castro, B. Anchoring of Copper(II) Acetylacetonate onto an Activated Carbon Functionalised with a Triamine. *Eur. J. Inorg. Chem.* **2004**, *2004*, 2027−2035.
(26) Vieira, R. S.; Oliveira, M. L. M.; Guibal, E.; Rodríguez-Castellón, E.; Beppu, M. M. Copper, mercury and chromium adsorption on natural and crosslinked chitosan films: An XPS investigation of mechanism. *Colloids Surf., A* **2011**, *374*, 108−114.
(27) Zhou, W.; Zhao, H.; Gao, J.; Meng, X.; Wu, S.; Qin, Y. Influence of a reagents addition strategy on the Fenton oxidation of rhodamine B: control of the competitive reaction of ·OH. *RSC Adv.* **2016**, *6*, 108791−108800.
(28) Li, J.-M.; Meng, X.-G.; Hu, C.-W.; Du, J.; Zeng, X.-C. Oxidation of 4-chlorophenol catalyzed by Cu(II) complexes under mild conditions: Kinetics and mechanism. *J. Mol. Catal. A: Chem.* **2009**, *299*, 102−107.
(29) Li, J.; Pham, A. N.; Dai, R.; Wang, Z.; Waite, T. D. Recent advances in Cu-Fenton systems for the treatment of industrial wastewaters: Role of Cu complexes and Cu composites. *J. Hazard. Mater.* **2020**, *392*, No. 122261.
(30) Lim, C. L.; Morad, N.; Teng, T. T.; Ismail, N. Treatment of Terasil Red R Dye Wastewater using H2O2/pyridine/Cu(II) System. *J. Hazard. Mater.* **2009**, *168*, 383−389.
(31) Pecci, L.; Montefoschi, G.; Cavallini, D. Some New Details of the Copper-Hydrogen Peroxide Interaction. *Biochem. Biophys. Res. Commun.* **1997**, *235*, 264−267.
(32) Fei, B.-L.; Wang, J.-H.; Yan, Q.-L.; Liu, Q.-B.; Long, J.-Y.; Li, Y.-G.; Shao, K.-Z.; Su, Z.-M.; Sun, W.-Y. Simple Copper(II) Schiff Base Complex as Efficient Heterogeneous Photo-Fenton-like Catalyst. *Chem. Lett.* **2014**, *43*, 1158−1160.
(33) Fei, B.-L.; Yan, Q.-L.; Wang, J.-H.; Liu, Q.-B.; Long, J.-Y.; Li, Y.-G.; Shao, K.-Z.; Su, Z.-M.; Sun, W.-Y. Green Oxidative Degradation of Methyl Orange with Copper(II) Schiff Base Complexes as Photo-Fenton-Like Catalysts. *Z. Anorg. Allg. Chem.* **2014**, *640*, 2035−2040.
(34) Watanabe, T.; Koller, K.; Messner, K. Copper-dependent depolymerization of lignin in the presence of fungal metabolite, pyridine. *J. Biotechnol.* **1998**, *62*, 221−230.
(35) Sigel, H.; Flierl, C.; Griesser, R. Metal ions and hydrogen peroxide. XX. On the kinetics and mechanism of the decomposition of hydrogen peroxide, catalyzed by the Cu2+-2,2′-bipyridyl complex. *J. Am. Chem. Soc.* **1969**, *91*, 1061−1064.
(36) Robbins, M. H.; Drago, R. S. Activation of Hydrogen Peroxide for Oxidation by Copper(II) Complexes. *J. Catal.* **1997**, *170*, 295−303.
(37) Baldrian, P.; Cajthaml, T.; Merhautová, V.; Gabriel, J.; Nerud, F.; Stopka, P.; Hrubý, M.; Beneš, M. J. Degradation of polycyclic aromatic hydrocarbons by hydrogen peroxide catalyzed by heterogeneous polymeric metal chelates. *Appl. Catal., B* **2005**, *59*, 267−274.
(38) Wang, Q.; Liang, S.; Zhang, G.; Su, R.; Yang, C.; Xu, P.; Wang, P. Facile and rapid microwave-assisted preparation of Cu/Fe-AO-PAN fiber for PNP degradation in a photo-Fenton system under visible light irradiation. *Sep. Purif. Technol.* **2019**, *209*, 270−278.
(39) Li, F.; Dong, Y.; Kang, W.; Cheng, B.; Qu, X.; Cui, G. Coordination Kinetics of Different Metal Ions with the Amidoximated Polyacrylonitrile Nanofibrous Membranes and Catalytic Behaviors of their Complexes. *Bull. Korean Chem. Soc.* **2016**, *37*, 1934−1941.
(40) Ahmed, A. H.; Thabet, M. S. Metallo-hydrazone complexes immobilized in zeolite Y: Synthesis, identification and acid violet-1 degradation. *J. Mol. Struct.* **2011**, *1006*, 527−535.
(41) Lázaro-Martínez, J. M.; Lombardo Lupano, L. V.; Piehl, L. L.; Rodríguez-Castellón, E.; Campo Dall' Orto, V. New Insights about the Selectivity in the Activation of Hydrogen Peroxide by Cobalt or Copper Hydrogel Heterogeneous Catalysts in the Generation of Reactive Oxygen Species. *J. Phys. Chem. C* **2016**, *120*, 29332−29347.
(42) Li, Y.; Yi, Z.; Zhang, J.; Wu, M.; Liu, W.; Duan, P. Efficient degradation of Rhodamine B by using ethylenediamine−CuCl2 complex under alkaline conditions. *J. Hazard. Mater.* **2009**, *171*, 1172−1174.
(43) Rao, K. S.; El-Hami, K.; Kodaki, T.; Matsushige, K.; Makino, K. A novel method for synthesis of silica nanoparticles. *J. Colloid Interface Sci.* **2005**, *289*, 125−131.

https://doi.org/10.1021/acsomega.2c03770
ACS Omega 2022, 7, 33258−33265